

The structure of oxygen-induced reconstruction on $\text{Cu}\{100\}$ - $c(2\times 2)$ -Pt surface alloy: the $\text{Pt}/\text{Cu}\{100\}$ - (2×2) -O

Ehab AlShamaileh ^{a,*}, Katariina Pussi ^b, Hamid Younis ^c,
Colin Barnes ^{c,*}, Matti Lindroos ^b

^a School of Physical Sciences, Dublin City University, Dublin 9, Ireland

^b Institute of Physics, Tampere University of Technology, P.O. Box 692, Tampere, Finland

^c School of Chemical Sciences, Dublin City University, Dublin 9, Ireland

Received 13 June 2003; accepted for publication 7 November 2003

Abstract

Adsorption of 0.25 ML oxygen on the $\text{Cu}\{100\}$ - $c(2\times 2)$ -Pt surface alloy followed by a brief thermal activation to 500 K and recooling to room temperature leads to the formation of a surface structure with a $p(2\times 2)$ periodicity. The structure of this $\text{Pt}/\text{Cu}\{100\}$ - (2×2) -O has been determined by quantitative low energy electron diffraction (LEED) calculations using the symmetrised automated tensor LEED (SATLEED) program. The results of the calculations suggest that simple $p(2\times 2)$ overlayers can be ruled out in favour of an oxygen-induced surface reconstruction. The favoured model (Pendry R -factor = 0.23) consists of a mixed $c(2\times 2)$ CuPt underlayer below a reconstructed $\text{Cu}\{100\}$ outermost layer with oxygen atoms occupying a slightly displaced fourfold hollow sites above second layer Pt atoms relative to the original unreconstructed surface.

© 2003 Elsevier B.V. All rights reserved.

Keywords: Surface relaxation and reconstruction; Surface structure, morphology, roughness, and topography; Alloys; Copper; Platinum; Oxygen; Chemisorption

Large mass reconstructions, in particular missing row reconstructions, induced by alkali adsorbates or oxygen are widely known on $\text{fcc}\{110\}$ surfaces. The existence of such reconstructions on $\text{fcc}\{100\}$ surfaces, where reconstruction of this type lowers the surface symmetry (this symmetry lowering does not happen in the $\text{fcc}\{110\}$ case),

sounds less presumable. One example of adsorbate-induced reconstruction on $\text{fcc}\{100\}$ is the missing-row $\text{Cu}\{100\}$ - $(2\sqrt{2}\times\sqrt{2})R45^\circ$ -2O reconstruction, first proposed by Zeng and Mitchell [1]. The $\text{Cu}\{100\}$ /O system has received much attention, especially the $\text{Cu}\{100\}$ - $c(2\times 2)$ -O phase [2], which is now known not to exist or at least not to be very stable. The structure of the $\text{Cu}\{100\}$ - $(2\sqrt{2}\times\sqrt{2})R45^\circ$ -O phase formed by the adsorption of 0.5 ML oxygen on $\text{Cu}\{100\}$ has been the subject of many studies [3–5]. LEED calculations revealed that this structure is a missing row reconstruction model, where every fourth row top layer atoms in

* Corresponding author. Tel.: +353-1-7005732; fax: +353-1-7005384.

E-mail address: ehab@dcu.ie (E. AlShamaileh).

* Deceased.

the [001] direction are missing. Oxygen is adsorbed on both sides of the missing row, almost co-planar with the copper, along the step edges and large expansion in the first interlayer spacing of the copper substrate is observed. Buckling and lateral displacement are also observed in the first two copper layers. The driving force in oxygen-induced reconstruction on copper surfaces is believed to be the formation of Cu–O–Cu chains [6].

The adsorption of oxygen on Cu{100}-c(2×2)-Pt 1 ML surface alloy produces a p(2×2) surface structure which we describe as oxygen-induced reconstruction. Recently, the structure and compositional profile of the Cu{100}-c(2×2)-Pt 1 ML surface alloy has been determined by AlShamaileh et al. [7]. The favoured model was an ordered c(2×2) CuPt underlayer below a Cu terminated surface where models involving a mixed ordered CuPt layer outermost may be definitively ruled out. The outermost three interlayer spacings were found to be expanded relative to the Cu{100} bulk value and a slight rippling was detected in the c(2×2) CuPt underlayer, with Pt atoms rippled outwards towards the vacuum interface within the composite layer.

In the present study, the effect of oxygen adsorption on the Cu{100}-c(2×2)-Pt 1 ML surface alloy structure is investigated.

All experiments were performed in an ion and titanium sublimation pumped ultra-high vacuum chamber equipped with facilities for LEED, AES and thermal desorption spectroscopy with a base pressure in the very low 10^{-10} Torr. A Quasar quadrupole mass spectrometer was available for residual gas analysis. The Cu{100} sample ($15 \times 10 \times 1.5$ mm) was mounted on a high precision goniometer allowing simultaneous motion in two orthogonal planes to allow accurate attainment of normal incidence. The sample could be heated by the resistive heating of four 0.25 mm Ta support wires with the sample temperature being monitored by a chromel–alumel thermo-couple embedded in a 0.25 mm diameter spark eroded hole through the top edge of the specimen. The sample was cleaned in situ by repeated cycles of argon ion bombardment (4 kV) and annealing to 700 K for 5 min periods. The clean Cu{100} sample showed no impurities by AES (C and O)

and exhibited a sharp well contrasted p(1×1) LEED pattern with normal incidence $I(V)$ spectra from the (1,0) beam in excellent visual agreement with previously reported spectra [8]. Platinum was evaporated from ultra-high purity (99.99%) 0.125 mm Pt wire wrapped around a shrouded and collimated 0.3 mm tungsten filament. The platinum evaporation rate was estimated by the periodic and simultaneous monitoring of the intensity and the full-width-at-half-maximum (f.w.h.m.) of the (1,0) and (1/2, 1/2) LEED reflexes as a function of Pt evaporation time. The Cu{100}-c(2×2)-Pt structure was formed by deposition of 1 ML of Pt onto Cu{100} with the sample held at room temperature, resulting in a high background LEED structure with weak broad c(2×2) reflexes. The procedure adopted to determine the optimal thermal treatment to form an optimally ordered c(2×2) surface alloy was as follows: a 1 ML Pt film was evaporated onto a clean Cu{100} surface at room temperature and a spot profile across the (1,0), (1/2, 1/2) and (0,1) beams was recorded. The surface was then heated to increasing temperature in increments of between 20 and 25 K with the crystal held at the anneal temperature for 1 min duration before cooling to a constant temperature and acquiring a spot profile. The optimal annealing temperature was decided by plotting both the integrated intensity and f.w.h.m. of the (1/2, 1/2) reflex as a function of annealing temperature: the optimal anneal temperature of 550 K was that required to bring the (1/2, 1/2) beam to a co-incident maximum intensity and minimum f.w.h.m. [9]. This method was adopted rather than traditional methods of coverage calibration such as construction of Auger signal versus deposition time plots due to Pt clustering and surface alloy formation which hinders exact coverage calibration by Auger spectroscopy.

The structure of the Pt/Cu{100}-(2×2)-O was prepared by dosing the Cu{100}-c(2×2)-Pt surface with over a 100 L oxygen (100 s exposure at a pressure of 10^{-6} Torr) and annealing to 550 K. This exposure is chosen to be higher than the saturation exposure on clean Cu{100} to ensure that a saturation coverage on the alloy is achieved. Higher exposures produced the same result. The annealing temperature of 550 K was found to give

the best $p(2 \times 2)$ LEED pattern upon oxygen adsorption. The formed $p(2 \times 2)$ phase exhibited sharp diffraction pattern indicating a long range ordered phase. For this phase, LEED $I(V)$ measurements were acquired at room temperature under conditions of normal incidence using a CCD video camera and collecting data by automatic spot tracking. Normal incidence was attained by variation of the sample alignment until the four $(1, 0)$ beams had identical spectral structure and highly similar relative intensities over the energy range 50–350 eV and over the whole period of the experiment. The $(1, 0)$ beam was remeasured at the end of the LEED $I(V)$ acquisition process to ensure the reproducibility of the spectra over the experiment's duration. Symmetry equivalent beams were co-added to reduce effects of residual sample misalignment. Prior to symmetry addition, each beam was individually background subtracted by fitting an exponential background to chosen minima in the $I(V)$ curves. The data was then normalised to constant incoming beam current. The data set utilised in the analysis consisted of seven symmetrically inequivalent beams and a total energy range of 1450 eV.

The calculations have been done using the Barbieri/Van Hove Symmetrised Automated Tensor LEED package [10]. Atomic potentials for Cu, Pt and O were characterised using 11 phase shifts ($I_{\max} = 10$) obtained from the Barbieri/Van Hove Phase Shift package [11]. Other non-structural parameters include Debye temperatures for copper, platinum and oxygen, which were set to fixed values at the beginning of the analysis (343, 240 and 600 K, respectively) and optimised at the end of analysis. Imaginary part of the inner potential was set to value -5 eV. The real part of inner potential was assumed to be energy independent and allowed to shift to obtain optimal theory experiment agreement as a standard procedure of LEED analysis. The theoretical intensities were calculated in energy range of 20–500 eV. The theory-experiment agreement was tested using Pendry reliability factor and error bars quoted has been calculated using Pendry RR -function [12]. Observed LEED pattern possess high symmetry of four mirror planes ($p4mm$). For the trial structures that have lower symmetry than $p4mm$,

proper domain averaging has been taken into account.

In addition to a model based on the previously determined $Cu\{100\}$ - $c(2 \times 2)$ -Pt unreconstructed surface alloy [7], the search was started by considering four different models exhibiting top layer reconstruction: a 25% decrease in surface Cu atoms density, a 50% decrease in surface Cu atoms density, a 75% decrease in surface Cu atoms density and a missing row model. For each of the five proposed models, oxygen atoms were placed in the high symmetry sites, namely: atop, hollow (above Cu), hollow (above Pt), bridge, or in the missing site where applicable. The models are illustrated in Fig. 1 and detailed in Table 1. For each of the models, the first step of the calculations involved varying the three dimensional oxygen atom positions and also varying the atomic positions of the first substrate layer. The composition of the substrate layers were fixed at the starting structure of the $Cu\{100\}$ /Pt surface alloy: pure copper in the topmost, third and deeper layers with the second layer being ordered $c(2 \times 2)$ CuPt. Due to the fact that many different possibilities of top layer reconstruction exist, a large number of trial structures had to be tested. All possible models with oxygen atoms adsorbed on high symmetry sites resulting in the $p(2 \times 2)$ periodicity were examined. The models and the tested adsorption sites along with their corresponding R_p -factors are listed in Table 1. With $R_p = 0.34$, this preliminary search clearly favours only one structure in which oxygen adsorbs on fourfold hollow sites above of second layer Pt of a 25% decrease in surface Cu atoms density reconstruction model (Fig. 1(b)).

Further refinement for the favoured model's second, third and fourth interlayer spacings was carried out. Phase shifts were calculated for this particular model and the Debye temperatures of the three elements were also optimised to finally give values of 250 K for surface copper, 343 K for second and deeper copper layers, 180 K for platinum and 300 K for oxygen. The imaginary part of the inner potential was allowed to vary and resulted in a value of -5 eV. It should be noted that further calculational refinement for all the structures with relatively low R_p -factor ($R_p < 0.45$ in Table 1) was performed as a double check

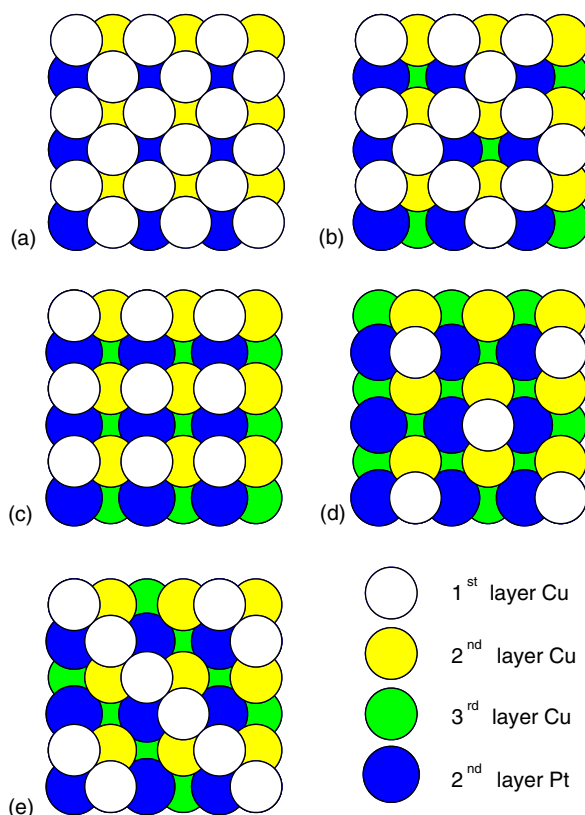


Fig. 1. Different structural models of top layer oxygen on CuPt surface alloy used in the preliminary stage of analysis. (a) Unreconstructed top layer, (b) 25% decrease in surface Cu atoms density, (c) 50% decrease in surface Cu atoms density, (d) 75% decrease in surface Cu atoms density and (e) missing row reconstruction. For a colour version of this figure, see the online paper.

procedure but no sign of other possible structures was concluded.

The refinement process leading to the determination of the compositional profile of this model was performed using the average T -matrix approximation (ATA) which allows variable Pt concentrations to be introduced into both the outermost layer and deeper into the selvedge (layers 3 and 4). Platinum was added in the form of a random substitutionally disordered $\text{Cu}_x\text{Pt}_{1-x}$ alloy into the first, second, third and fourth layers in steps of 10% in the range of 0–40%. The optimum compositional profile was finally achieved with a 20 ± 20 at.% Pt in the first layer and 10 ± 10 at.% Pt in the fourth layer while the second layer composition for this model is found to be CuPt. The use of the ATA approach resulted in a further

reduction of the Pendry R_p -factor for the favoured model (final $R_p = 0.23$).

The compositional profile in the presence of oxygen changes from that of the $\text{Cu}\{100\}\text{-c}(2 \times 2)\text{-Pt}$ 1 ML alloy in which a composition of 5 ± 5 at.%, 20 ± 20 at.% and 30 ± 30 at.% was favoured for the first, third and fourth layers respectively (second layer was also an ordered $\text{c}(2 \times 2)$ CuPt layer) [7]. Hence, substrate structural changes were induced by the oxygen adsorption. The most notable change is the reconstruction of the top layer of the substrate expressed by a decrease of 25% of the surface Cu atoms density. Adsorbate induced reconstruction on some surfaces is known to take place via breaking and creating substrate–substrate or substrate–adsorbate bonds mainly by changing the atomic density

Table 1
Pendry R -factors from the preliminary state of analysis

Model	Site	R_p
Unreconstructed surface (Fig. 1(a))	Top	0.58
	Hollow (Cu)	0.46
	Hollow (Pt)	0.53
	Bridge	0.70
25% Decrease in surface density (Fig. 1(b))	Top	0.51
	Hollow (Cu)	0.44
	Hollow (Pt)	0.34
	Bridge	0.41
	Missing top	0.40
	ATA	0.41
50% Decrease in surface density (Fig. 1(c))	Top	0.55
	Hollow (Cu)	0.56
	Hollow (Pt)	0.45
	Bridge	0.50
	Missing top	0.42
75% Decrease in surface density (Fig. 1(d))	Top	0.57
	Hollow (Cu)	0.50
	Hollow (Pt)	0.50
	Bridge	0.47
	Missing top	0.48
	ATA	0.46
Missing row (Fig. 1(e))	Top	0.65
	Hollow (Cu)	0.41
	Hollow (Pt)	0.42
	Bridge	0.55
	Missing top	0.57
	Missing bridge	0.47

ATA corresponds to structures were $p(2 \times 2)$ periodicity comes from the surface reconstruction and 0.25 ML oxygen was substituted into the top layer as a disordered alloy.

of the top layer [13]. In the case of oxygen on CuPt surface alloy, the decrease in the top layer copper density may be explained by the tendency to form stronger Cu–O bonds since top layer copper atoms have fewer nearest neighbours which probably increases the charge transfer between copper and oxygen atoms. The adsorption of oxygen in the hollow sites produces local Cu–O–Cu chains since oxygen has two nearest neighbour Cu atoms to which it can bond. The shortest Cu–O bond is found to be $2.0 \pm 0.2 \text{ \AA}$, which compares well with Cu–O bond length in the CuO structure (1.95 \AA). The shortest Pt–O bond is found to be $2.1 \pm 0.2 \text{ \AA}$, which is similar to the Cu–O bond within the error bars of the calculation. Copper and oxygen atoms in the top layer are almost co-planar with oxygen

being 0.03 and $0.10 \pm 0.13 \text{ \AA}$ higher than the two inequivalent copper atoms in the first substrate layer.

With respect to the $\text{Cu}\{100\}$ bulk structure, the first two interlayer spacings (dz_{12} and dz_{23}) are both largely expanded by $5 \pm 1\%$ while the third interlayer spacing is slightly expanded by $1 \pm 1\%$. Compared to the $\text{Cu}\{100\}$ - $c(2 \times 2)$ -Pt surface alloy, the changes in the interlayer spacing are found to consist of an expansion of $3 \pm 1\%$ in the first interlayer spacing and of a contraction of $1 \pm 1\%$ and $3 \pm 3\%$ in second (dz_{23}) and third (dz_{34}) interlayer spacing, respectively. The large expansion in the first interlayer spacing (dz_{12}) is attributed to the direct effect of oxygen adsorption and oxygen-induced surface reconstruction. All interlayer

spacing values in this study are quoted between copper atoms in the different layers or between their centre of mass for layers with inequivalent Cu atoms.

A buckling in the topmost copper layer where two inequivalent copper atoms exist was found to be 0.07 ± 0.03 Å. Platinum atoms in the second layer are buckled by -0.13 ± 0.04 Å and $+0.04 \pm 0.04$ Å (The $-$ sign corresponds to relaxation towards the solid vacuum interface and the $+$ sign to relaxation away from the solid vacuum interface.) relative to second layer Cu atoms. The average buckling measured from the centre of mass of copper atoms in the third and fourth layers are 0.01 ± 0.05 Å and 0.02 ± 0.05 Å, respectively. The calculations revealed a small lateral displacement of 0.05 ± 0.06 Å, observed in the topmost layer copper atoms whereas larger values of 0.23 ± 0.12 Å and 0.11 ± 0.12 Å were observed for the second layer platinum atoms. Oxygen atoms were found to be displaced by 0.8 ± 0.2 Å within the plane of the topmost layer towards the position of the missing surface Cu atom as illustrated in Fig. 2(a). Fig. 2 is a schematic diagram showing top and side views of the optimum structure. The main geometric parameters are summarised in Table 2.

The observed lateral displacements are a direct result of the LEED $I(V)$ simulations. Other spectroscopic techniques are needed to confirm and possibly explain the oxygen-induced lateral displacements on the surface of a nearly stable Cu-capped CuPt surface alloy (Fig. 3).

Using low energy ion scattering, recoiling spectrometry and low energy electron diffraction, Shen et al. have studied the oxygen induced (2×1) reconstruction of $\text{Cu}_3\text{Pt}\{110\}$ [14]. In that study, oxygen is found to induce a missing row type reconstruction where every second row in the $[100]$ direction is missing. The first interlayer spacing was found to expand by $23 \pm 10\%$ with respect to an ideally terminated $\text{Cu}_3\text{Pt}\{110\}$ surface. Oxygen was adsorbed on bridge sites, 0.1 ± 0.1 Å below the missing row copper atoms, to form chains of Cu–O–Cu in the $[100]$ direction. Oxygen was found to bond to four copper atoms, two in the first layer (Cu–O bond length 1.85 ± 0.15 Å) and two in second layer (Cu–O bond length 1.99 ± 0.20 Å).

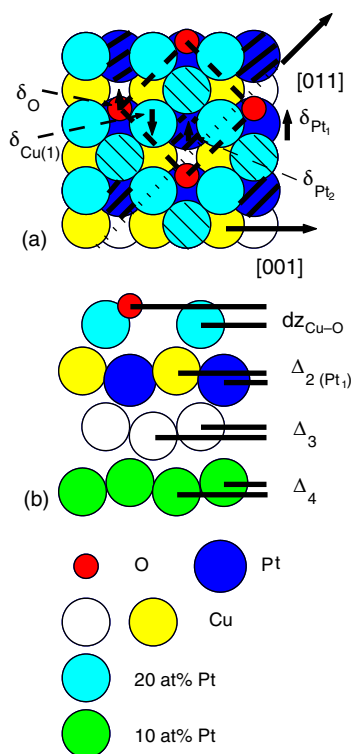


Fig. 2. (a) Top view of the favoured structure. Unit cell is shown with dashed line and main crystallographic directions are indicated. (b) Side view along dotted line ($[011]$ direction) in Fig. 2(a). Buckling and interlayer spacings are drawn overestimated for clarity. Note that all atoms are not in the same plane. In the top two layers, shaded Cu and Pt atoms indicate the presence of inequivalent atoms within the same layer. For a colour version of this figure, see the online paper.

We note that the reconstruction effect of oxygen is much greater on the Cu_3Pt alloy compared to the CuPt underlayer surface alloy. This may be due to the very different composition of the topmost layer of each surface and also to the concentration of Pt atoms in the selvedge. The results of this study are of importance to reactions that involve oxidation processes on mixed CuPt surfaces.

Finally, the relatively high R -factor value (0.23) is considered reasonable for a system with three different atoms within the selvedge. For the clean $\text{Cu}\{100\}$ surface, the total R -factor measured in our lab was 0.15 [8] while for the underlayer structure of the $\text{Cu}\{100\}$ - $c(2 \times 2)$ -Pt it was 0.20 [7]. Hence, a slightly higher value is not unexpected for the more complicated structure inves-

Table 2
Main structural parameters for the optimum structure

Parameter ^a	Value (Å)
$d_{\text{Cu-O}}$	2.0 ± 0.2
$d_{\text{Pt-O}}$	2.1 ± 0.2
$dz_{\text{Cu-O}}$	$0.03/0.10 \pm 0.13$
Δ_1	0.07 ± 0.03
Δ_2 (Pt ¹)	0.13 ± 0.04
Δ_2 (Pt ²)	0.04 ± 0.04
Δ_3	0.01 ± 0.05
Δ_4	0.02 ± 0.05
dz_{12}	1.89 ± 0.02
dz_{23}	1.89 ± 0.02
dz_{34}	1.83 ± 0.04
δ_{O}	0.8 ± 0.2
$\delta_{\text{Cu}(1)}$	0.05 ± 0.12
δ_{Pt_1}	0.11 ± 0.12
δ_{Pt_2}	0.23 ± 0.12

^a $d_{\text{Cu-O}}$ is the nearest-neighbour Cu–O bond, $d_{\text{Pt-O}}$ is the nearest-neighbour Pt–O bond, $dz_{\text{Cu-O}}$ is the vertical distance between oxygen and top layer Cu atoms, Δ_1 is the buckling in the first layer Cu atoms, Δ_2 (Pt¹) and Δ_2 (Pt²) are the buckling in the second layer Pt atoms with respect to second layer Cu atoms, Δ_3 is the average buckling in the third layer Cu atoms, Δ_4 is the average buckling in the fourth layer Cu atoms, Interlayer spacing values (dz_{12} , dz_{23} and dz_{34}) are quoted between Cu atoms or between their centre of mass with layers of inequivalent Cu atoms. δ_{O} is the lateral displacement of oxygen atoms, $\delta_{\text{Cu}(1)}$ is the lateral displacement of Cu atoms in the topmost layer and δ_{Pt_1} and δ_{Pt_2} represent the lateral displacement of the two different second layer Pt atoms. The different geometrical parameters can be visualised with the aid of Fig. 2.

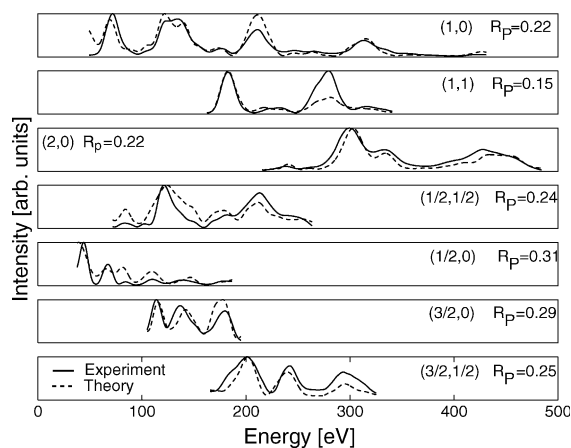


Fig. 3. Optimal theory-experiment agreement. Experimental data is shown as full lines and theory as dotted lines.

tigated in this study. A high R -factor may indicate the presence of surface disorder or the co-existence

of regions with different structures in the course of the CuPt underlayer alloy formation process (e.g. $(1 \times 1) + c(2 \times 2)$ phases).

It is interesting to analyse the changes in the symmetry of the different structures tested in this study. In Contrast to fcc $\{110\}$ surfaces, symmetry reduction is an evident consequence of the surface reconstruction on fcc(100) surfaces [15]. In our case, the symmetry of the unreconstructed CuPt(100) underlayer alloy is p4mm. For the different top layer reconstruction models tested in this study, the surface symmetry is reduced to either p2mm or p2. In the models exhibiting a reduction of 25%, 50% and 75% in the surface Cu atoms density, the symmetry is reduced to p2mm while in the missing row surface reconstruction the surface symmetry it is reduced to p2. The tendency for possessing higher symmetry in the reconstruction process adds an additional support to the result that the model with 25% decrease in surface Cu atoms density is favoured over the missing row reconstruction model in the CuPt(100)–O underlayer system.

Adsorption of oxygen on the Cu $\{100\}$ - $c(2 \times 2)$ -Pt 1 ML surface alloy induces significant reduction in the surface Cu atoms density and produces a structure exhibiting a $p(2 \times 2)$ periodicity. This change of the surface structure and compositional profile of the surface alloy may be explained by the formation of Cu–O chains. The geometric structure has been determined using the SATLEED calculations. The calculations ruled out simple $p(2 \times 2)$ overlayers in favour of an oxygen-induced surface reconstruction model that consists of a mixed $c(2 \times 2)$ CuPt underlayer below a reconstructed Cu $\{100\}$ outermost layer with oxygen atoms occupying a slightly displaced fourfold hollow sites above second layer Pt atoms relative to the Cu $\{100\}$ - $c(2 \times 2)$ -Pt unreconstructed surface. The minimum Pendry R -factor for the best model was 0.23.

Acknowledgements

K.P. would like to thank the Finnish National Graduate School in Material Physics (NGSMP) for financial support.

References

- [1] H.C. Zeng, R.A. McFarlane, R.N.S. Sodhi, K.A.R. Mitchell, *Can. J. Chem.* 66 (1988) 2054.
- [2] U. Döbler, K. Baberschke, J. Stöhr, D.A. Outka, *Phys. Rev. B* 31 (1985) 2532.
- [3] A. Atrei, U. Bardi, G. Rovida, E. Zanazzi, G. Casalone, *Vacuum* 41 (1990) 333.
- [4] H.C. Zeng, R.A. McFarlane, K.A.R. Mitchell, *Surf. Sci.* 208 (1989) L7.
- [5] J.H. Onuferko, D.P. Woodruff, *Surf. Sci.* 95 (1980) 555.
- [6] C.Q. Sun, *Surf. Rev. Lett.* 8 (2001) 367, and references therein.
- [7] E. AlShamaileh, H. Younis, C.J. Barnes, K. Pussi, M. Lindroos, *Surf. Sci.* 515 (2002) 94.
- [8] E. AlShamaileh, C.J. Barnes, *Phys. Chem. Chem. Phys.* 4 (2002) 5148.
- [9] J.P. Reilly, D. O'Connell, C.J. Barnes, *J. Phys.: Condens. Matter* 11 (1999) 417.
- [10] M.A. Van Hove, W. Moritz, H. Over, P.J. Rous, A. Wander, A. Barbieri, N. Materer, U. Starke, G.A. Somorjai, *Surf. Sci. Rep.* 19 (1993) 191.
- [11] A. Barbieri, M.A. Van Hove, private communication.
- [12] J.B. Pendry, *J. Phys. C: Solid State Phys.* 13 (1980) 937.
- [13] V. Fiorentini, M. Methfessel, M. Scheffler, *Phys. Rev. Lett.* 71 (1993) 1051.
- [14] Y.G. Shen, D.J. O'Connor, K. Wandelt, *Surf. Sci.* 410 (1998) 1.
- [15] D.P. Woodruff, in: D.A. King, D.P. Woodruff (Eds.), *The Chemical Physics of Solid Surfaces*, Elsevier, 1994, p. 465.